Time-Frequency Analysis for the Localization of Multiple Moving Targets Using Dual-Frequency Radars

Yimin Zhang, *Senior Member, IEEE*, Moeness Amin, *Fellow, IEEE*, and Fauzia Ahmad, *Senior Member, IEEE*

***Abstract*—A dual-frequency radar, which estimates the range of a target based on the phase difference between two closely spaced frequencies, has been shown to be a cost-effective approach to accomplish both range-to-motion estimation and tracking. This approach, however, suffers from two drawbacks: it cannot deal with multiple moving targets, and it has poor performance in noisy environments. In this letter, we propose the use of time-frequency signal representations to overcome these drawbacks. The phase, and subsequently the range information, is obtained based on the moving target instantaneous Doppler frequency law, which is provided through time-frequency signal representations. The case of multiple moving targets is handled by separating the different Doppler signatures prior to phase estimation.**

***Index Terms*—Dual-frequency radar, moving target localization, time-frequency analysis.**

I. Introduction

THROUGH-THE-WALL radar (TWR) imaging and sensing is an emerging technology supporting a range of civilian and military applications [1]–[6]. TWR has been recently sought out for surveillance and reconnaissance in urban environments, requiring not only the layout of the building, including types and locations of walls, but also detection and localization of both moving and stationary targets within enclosed structures. This technology can also be used by firefighters to detect and locate survivors, by law enforcement officers for enhanced situational awareness and tailored tactical operations, and in search and rescue operations in natural disasters.

Doppler radars exploiting continuous-wave (CW) waveforms are often used in the detection of moving targets due to their cost effectiveness [6]–[8]. Because Doppler radars typically use a single frequency, they are impractical for estimating the range of a target. A simple and low-cost alternative is to use dual-frequency CW radar, which employs two different frequencies and simultaneously measures the phase change with respect to time, for each of the two frequencies. The range is estimated based on the phase difference between the two frequencies [9]–[12]. Due to phase wrapping in the observation of return signals, there exists the range ambiguity problem. The maximum unambiguous range of the target is determined by the separation between the two distinct carrier frequencies. In urban sensing, this unambiguous range may be sufficient to uniquely solve for the target range, given prior knowledge of the structure bounds on target location. For example, a 10-MHz difference in the carrier frequencies yields an unambiguous range of 15 m.

The performance of the dual-frequency radar technique rapidly degrades when operating in a noisy environment [11], which is commonly encountered in urban sensing applications, or when dealing with multiple targets. In the latter, the received signal is the superposition of returns from different targets, and therefore, phase information corresponding to individual targets cannot be obtained from the raw data. Similarly, when there are strong multipaths, the phase information is distorted and does not yield correct range estimates.

In this letter, we propose the use of time-frequency representation of the target return signals for improved range estimation and tracking of one or more moving targets. The proposed technique has three major advantages. First, the time-frequency representation allows concentration of the signal energy around the instantaneous Doppler frequency and thus enhances the signal-to-noise ratio (SNR) [13]. Second, time-frequency representations provide a platform to obtain enhanced phase information as well as the Doppler signatures of the targets. Thus, range estimation and tracking can be improved through the fusion of Doppler signature and the phase information, which is most effective, particularly in low SNR scenarios. Third, separation of multiple target signals can be accomplished in the time-frequency domain.

II. Concept of Dual-Frequency CW Radar

Consider a dual-frequency CW radar operating at frequencies f_1 and f_2. The baseband radar return at the two frequencies can be expressed as

$$s_i(t) = \rho_i(t) \exp(-j\phi_i(t)), \quad i = 1,\, 2 \tag{1}$$

where $\rho_i(t)$ and $\phi_i(t) = 4\pi f_i R(t)/c$ are, respectively, the range-dependent amplitude and the phase of the return corresponding to the ith frequency of operation, c is the velocity of wave propagation, and $R(t)$ is the range of the moving target.

Manuscript received July 21, 2008; revised September 20, 2008. This work was supported in part by ONR under grant N00014-07-1-0043 and in part by DARPA under contract no. HR0011-06-C-0110. The content of the information does not necessarily reflect the position or the policy of the Government, and no official endorsement should be inferred. Approved for Public Release, Distribution Unlimited. This work was presented in part at the Annual Asilomar Conference on Signals, Systems, and Computers, Pacific Grove, CA, Nov. 2007. The associate editor coordinating the review of this manuscript and approving it for publication was Prof. Behrouz Farhang-Boroujeny.

The authors are with the Center for Advanced Communications, Villanova University, Villanova, PA 19085 USA (e-mail: yimin.zhang@villanova.edu; moeness.amin@villanova.edu; fauzia.ahmad@villanova.edu).

Color versions of one or more of the figures in this paper are available online at http://ieeexplore.ieee.org.

Digital Object Identifier 10.1109/LSP.2008.2008213

Without considering phase wrapping, range $R(t)$ can be estimated from the phase difference observed at the return signal corresponding to the two frequencies, i.e.,

$$R(t) = \frac{c[\phi_2(t) - \phi_1(t)]}{4\pi(f_2 - f_1)}. \quad (2)$$

In reality, however, phase observations are wrapped within the $[0, 2\pi)$ range. Therefore, the true phase can be expressed as

$$\phi^{(true)}(t) = \phi_2(t) - \phi_1(t) + 2m\pi \quad (3)$$

where m is an unknown integer. Accordingly, the range estimate is subject to range ambiguity [9], [11], i.e.,

$$R(t) = \frac{c[\phi_2(t) - \phi_1(t)]}{4\pi(f_2 - f_1)} + \frac{cm}{2(f_2 - f_1)}. \quad (4)$$

The second term in the above equation induces ambiguity in range. For the same phase difference, the range can assume infinite values separated by

$$R_{\max} = \frac{c}{2(f_2 - f_1)} \quad (5)$$

which is referred to as the maximum unambiguous range.

III. Range Estimation Based on Time-Frequency Representation

A. Short-Time Fourier Transform

We exploit the short-time Fourier transform (STFT) to demonstrate the effectiveness of time-frequency analysis to provide enhanced range estimates of moving targets using a dual-frequency radar. The STFT of a signal $x(t)$ can be defined as

$$F_x(t, f) = \int_{-\infty}^{\infty} x(\tau)h(\tau - t)e^{-j2\pi f\tau}d\tau \quad (6)$$

where $h(t)$ is the window function. The use of different windows allows trading-off the time and frequency resolutions.

B. Range Estimation Based on STFT Phase Information

The Doppler frequency shift, $f_{D,i}(t)$, of a moving target is the differential of the corresponding phase. For a signal waveform expressed in (1), $f_{D,i}(t)$ can be obtained as

$$f_{D,i}(t) = -\frac{1}{2\pi}\frac{d\phi_i(t)}{dt} = -\frac{2f_i}{c}\frac{dR(t)}{dt}. \quad (7)$$

As discussed earlier, the phase information, and thereby the range estimate, obtained at the Doppler signatures in the time-frequency domain is much more robust to noise as compared to that obtained from the raw data due to SNR enhancement. In addition, multiple target returns with distinct Doppler signatures can be separated in the time-frequency domain. With the ability of capturing the Doppler signature of each moving target in the scene, one can proceed to calculate the respective phase information and, subsequently, estimate the target range.

The selection of the Doppler signatures in the time-frequency domain, in general, can be done using simple peak detection. With multiple moving targets, some additional work may be required to trace different segments of the Doppler signature of the same target. Separation of non-overlapping and crossing Doppler signatures can be effectively performed by observing phase continuity [14], often describing motions of indoor animate or inanimate target.

The effect of multipath, which is a common occurrence in a typical urban sensing environment, may also distort the phase of return signals. In a propagation environment with two or more paths, the phase of the received signal corresponds to neither the target (direct path) nor that of the indirect path. When the direct and indirect paths have distinct Doppler signatures (e.g., a reflector behind a target generates Doppler frequency opposite to that of the direct path), they can be well separated and discriminated in the time-frequency domain.

C. Range Estimation Based on Doppler Signatures

In addition to the phase information, the Doppler signature of each target can also be obtained from the time-frequency representations. From (7), we obtain

$$\phi_i(t) = \phi_i(0) - 2\pi\int_0^t f_{D,i}(t)dt. \quad (8)$$

The phase difference $\phi(t) = \phi_2(t) - \phi_1(t)$ is important for range estimation. From (7), it is known that the Doppler frequency shift is proportional to the carrier frequency, resulting in the following relationship:

$$f_{D,2}(t) - f_{D,1}(t) = \left(\frac{f_2}{f_1} - 1\right) f_{D,1}(t). \quad (9)$$

Thus

$$\begin{aligned}\phi(t) &= \phi(0) - 2\pi\int_0^t [f_{D,2}(t) - f_{D,1}(t)]dt \\ &= \phi(0) - 2\pi\left(\frac{f_2}{f_1} - 1\right)\int_0^t f_{D,1}(t)dt. \quad (10)\end{aligned}$$

As such, the phase information of the return signals and, subsequently, the ranges of moving targets, can be obtained from the Doppler frequency shift up to an initial value. The unknown initial phase difference $\phi(0)$ can be estimated by minimizing the overall distance between $\phi(t)$, obtained from (10), and the phase difference directly obtained from the phase of the STFT, $\tilde{\phi}(t) = \tilde{\phi}_2(t) - \tilde{\phi}_1(t)$, at the selected Doppler signatures. That is

$$\phi(0) = \arg\min_{\phi(0)} \int \|\phi(t) - \tilde{\phi}(t)\|^2 dt \quad (11)$$

where the integral is evaluated over the entire observation period. Both simulation and experiment results have shown that range estimates based on the Doppler signature are robust to various perturbation factors caused by noise, reflections, and cross-component interference, compared to those obtained from raw data or from directly using the corresponding phase value in

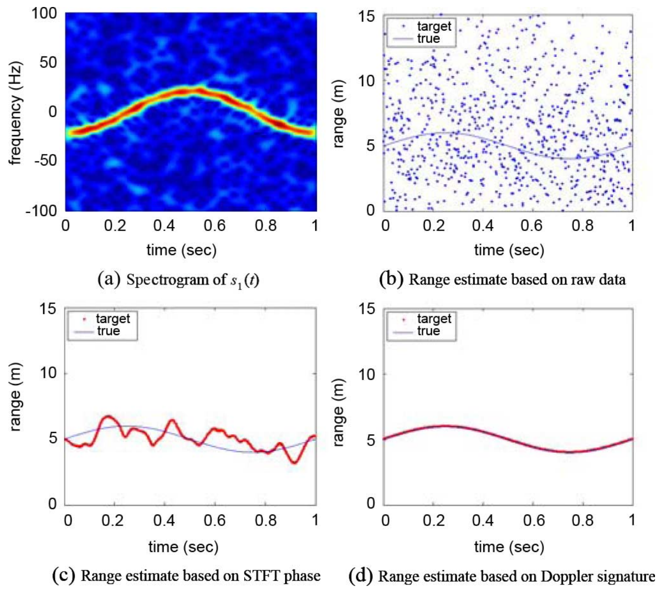

(a) Spectrogram of $s_1(t)$ (b) Range estimate based on raw data

(c) Range estimate based on STFT phase (d) Range estimate based on Doppler signature

Fig. 1. STFT and range estimation results of a single target case in the presence of noise (SNR $= 0$ dB).

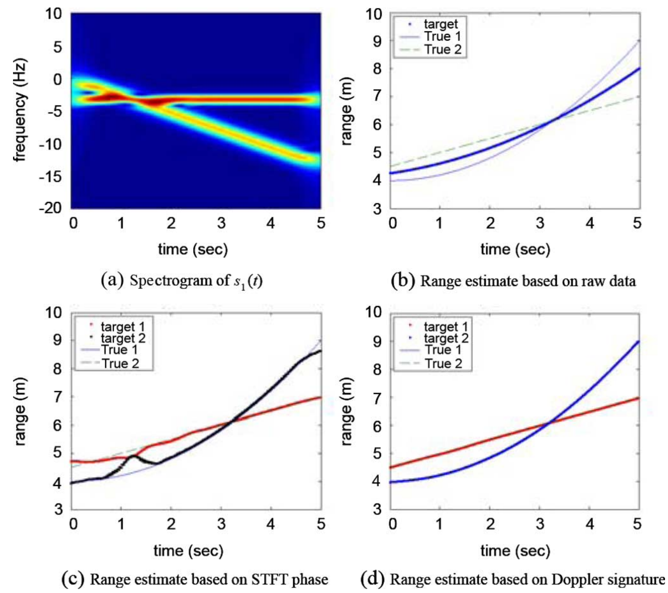

(a) Spectrogram of $s_1(t)$ (b) Range estimate based on raw data

(c) Range estimate based on STFT phase (d) Range estimate based on Doppler signature

Fig. 2. STFT and range estimates of two-targets in the absence of noise. The targets have overlapping Doppler signatures in the time-frequency domain.

the STFT. Note that a Doppler signature bias may accumulate over time to yield a large error in the range estimate. Therefore, high-frequency resolution is desirable in computing the STFT.

IV. Simulation Results

We first consider a single target scenario. The target swings around a center which is 5 m away from the radar with a maximum displacement of 1 m. The observation period is 1 s. The two carrier frequencies are 990 MHz and 1 GHz, respectively. The reflection coefficient is assumed to be a constant, regardless of the range. The input SNR is 0 dB.

Fig. 1(a) shows the spectrogram of $s_1(t)$. Due to the frequency resolution limitation, the STFT signature of $s_2(t)$ approximately coincides with that of $s_1(t)$. The sampling frequency is 1 kHz, and a 101-point Hanning window is used. As shown in Fig. 1(a), despite the low SNR level, the Doppler frequency signatures can be clearly identified in the spectrogram. Fig. 1(b)–(d) shows the range estimates using raw data, STFT phase, and the Doppler signature. It is evident from Fig. 1(b) that, because of the noise, the raw data-based approach fails to provide meaningful range estimates. Significant improvement is achieved when using the phase information from the STFT. The best results are, however, obtained when the Doppler signature-based approach is applied. In this case, the range estimation error is very small.

Next, we consider a two-target scenario, where the Doppler frequencies of the two targets overlap. A target moves away from the radar at a constant speed of 0.5 m/s, whereas another target moves away at a time-varying speed, accelerating from 0 m/s to 2 m/s over the 5-s period. The initial ranges of the two targets are 4.5 m and 4 m, respectively. To clearly illustrate the effect of multiple targets, no noise is considered in this example. Fig. 2(a) shows the STFT results at the carrier frequency of 900 MHz. The Doppler frequencies of the two targets are separated in the time-frequency domain for most of the observation period, but they overlap at around $t = 0.125$ s. As a result, poor range estimates occur around this moment when the STFT phase information is used, as seen in Fig. 2(c). This problem is overcome by using the instantaneous Doppler signature, as demonstrated by the range estimate in Fig. 2(d). For comparison, we also show the results using raw data, which only yields a single estimated trajectory in the middle of the true target trajectories [Fig. 2(b)].

V. Experimental Results

To demonstrate the effectiveness of the proposed method in a real environment, experiments were conducted in a laboratory setting. A dual-frequency radar with operational frequencies of 919.866 MHz and 906.317 MHz was employed, and a ten-element Welded Yagi antenna was used. The walls of the lab were lined with electromagnetic absorbers to reduce ambient reflections. The received baseband data are preprocessed to remove clutter component near the dc frequency before time-frequency analysis and range estimation are performed.

In the first experiment, two conducting spheres of diameter 0.25 m and 0.20 m are mounted on separate linear positioners. One sphere remains stationary at the far end whereas the other moves back and forth over a 3.05-m range with a speed of 0.635 m/s. Thus, it takes approximately 4.8 s for the sphere to travel in one direction. The sampling frequency is 1 kHz and the time duration of the collected data is 20 s. Fig. 3(a) shows the spectrogram of the baseband signal corresponding to carrier frequency of 919.866 MHz, where a 2001-point Hanning window is used to perform an 8192-point STFT. The estimated range using raw data is shown in Fig. 3(b), whereas that estimated from the STFT phase difference is shown in Fig. 3(c). Note that, in this example, the SNR is relatively high. As a result, range estimation based on raw data is relatively acceptable, although some local variance is observed. Such variance is not observed in Fig. 3(c)–(d) for the result based on time-frequency representations. Interestingly, range estimation results in Fig. 3(b)–(c) are affected by

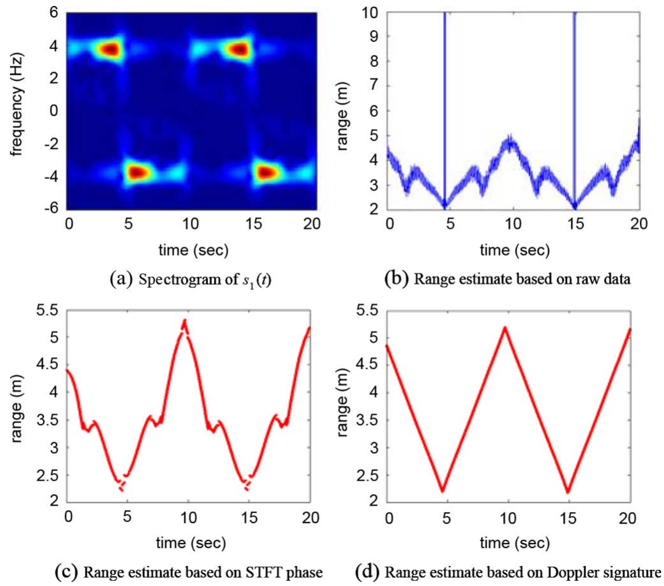

Fig. 3. STFT and range estimation results of the first experiment where one conducting sphere moves back and forth.

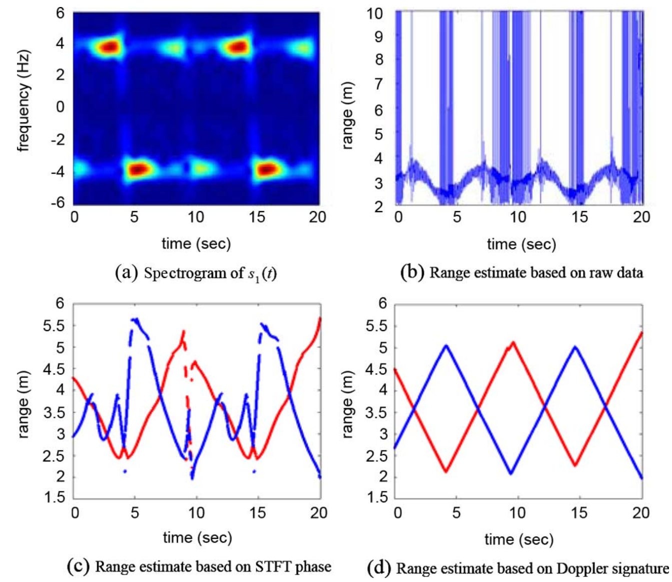

Fig. 4. STFT and range estimates of the second experiment where both conducting spheres move with the same speed but in opposite directions.

a phase distortion due to reflection from a computer rack located in the corner of the lab. The effect of the reflection is observed in Fig. 3(a) as a weak chirp. Such effect is mitigated when the Doppler signature-based approach is exploited, as shown in Fig. 3(d). This is a good example that demonstrates the capability of the proposed method to perform range estimation in a multipath environment. Nevertheless, the proposed method may not properly function in a complicated multipath environment where the Doppler signature of the targets corresponding to the direct path is overshadowed by the Doppler signature due to multipath.

The second experiment has the same setting as the first one, except that now both conducting spheres move with the same speed but in opposite directions. Fig. 4(a) shows the spectrogram of the baseband signal. When raw data are used, as shown in Fig. 4(b), only the range of the sphere closer to the radar at each time is obtained as its return signal has a dominative effect on the phase of the received signal. Time-frequency analysis-based methods allow separation of the two targets. The STFT phase-based method provides relatively good range estimates for the 0.25-m sphere, but the result for the 0.20 m is not consistent. The proposed Doppler signature-based approach yields very robust range estimation for both targets.

VI. Conclusions

The dual-frequency radar approach estimates the range of a moving target by estimating the phase difference of the signal returns at two closely spaced frequencies of operation. The performance of such a radar system degrades significantly in high noise power level and/or with multiple moving targets. To overcome these shortcomings, a technique based on determining the phase from the instantaneous frequency law of the target Doppler signature was proposed. This technique operates with enhanced SNR through time-frequency signal representations. It enables accurate range estimation in the presence of multiple targets as well as multipath propagation. Simulation and experimental results were provided to clearly demonstrate the capability of the proposed method.

References

[1] D. D. Ferris, Jr and N. C. Currie, “A survey of current technologies for through-the-wall surveillance,” in *Proc. SPIE*, San Diego, CA, Nov. 1998, vol. 3577, pp. 62–72.
[2] *Proc. 2004 IEEE AP-S Int. Symp., Special Session on Through-Wall Imaging,* Jul. 2004.
[3] *Digest of 2007 URSI North American Radio Science Meeting, Special Session on Through-Wall Imaging,* Jul. 2007.
[4] *Proc. 2008 IEEE ICASSP, Special Session on Through-the-Wall Radar Imaging,* Mar. 2008.
[5] S. S. Ram, Y. Li, A. Lin, and H. Ling, “Doppler-based detection and tracking of humans in indoor environments,” *J. Franklin Inst.*, vol. 345, no. 6, pp. 679–699, Sep. 2008.
[6] T. Thayaparan, L. Stankovic, and I. Djurovic, “Micro-Doppler human signature detection and its application to gait recognition and indoor imaging,” *J. Franklin Inst.*, vol. 345, no. 6, pp. 700–722, Sep. 2008.
[7] V. Chen, “Analysis of radar micro-Doppler signature with time-frequency transform,” in *Proc. IEEE Workshop Statistical Signal and Array Processing*, Pocono, PA, Aug. 2000.
[8] W. D. Boyer, “A diplex, Doppler, phase comparison radar,” *IEEE Trans. Aerosp. Navig. Electron.*, vol. ANE-10, no. 3, pp. 27–33, 1963.
[9] F. Ahmad, M. Amin, and P. Setlur, “Through-the-wall target localization using dual-frequency CW radars,” in *Proc. SPIE*, Orlando, FL, Apr. 2006, vol. 6201.
[10] A. Lin and H. Ling, “Three-dimensional tracking of humans using very low-complexity radar,” *Electron. Lett.*, vol. 42, no. 18, pp. 1062–1064, Aug. 2006.
[11] F. Ahmad, M. G. Amin, and P. D. Zemany, “Performance analysis of dual-frequency CW radars for motion detection and ranging in urban sensing applications,” in *Proc. SPIE*, Orlando, FL, Apr. 2007, vol. 6547.
[12] Y. Zhang, M. G. Amin, and F. Ahmad, “A novel approach for moving multi-target localization using dual frequency radars and time-frequency distributions,” in *Proc. Annu. Asilomar Conf. Signals, Systems, and Computers*, Pacific Grove, CA, Nov. 2007.
[13] Y. Zhang, W. Mu, and M. G. Amin, “Subspace analysis of spatial time-frequency distribution matrices,” *IEEE Trans. Signal Process.*, vol. 49, no. 4, pp. 747–759, Apr. 2001.
[14] A. Jarrot, C. Ioana, C. Gervaise, and A. Quinquis, “A time-frequency characterization framework for signals issued from underwater dispersive environments,” in *Proc. IEEE ICASSP*, Honolulu, HI, Apr. 2007, pp. III-1145–1148.